



May, 15th 2018, Nürnberg, Germany

Spatial distribution of nucleated bubbles in molten glasses undergoing coalescence and growth

D. Boloré (Surface du Verre et Interfaces, UMR 125 CNRS/Saint-Gobain)
& **F. Pigeonneau**



Industrial Context

- ▶ Cullet is mainly used for the production of container glass:

Germany	85 %	Belgium	96 %	France	75 %
Poland	57 %	Italy	78 %	Austria	87 %
United-Kingdom	66 %	Portugal	58 %	Spain	70 %
Sweden	99 %	Holland	83 %	Denmark	85 %

Table 1: Rates of glass recycling in Europe in 2015 [FEVE source].

- ▶ Advantages of introduction of cullet in raw materials:
 - ▶ Reductions of mineral resources;
 - ▶ Reduction of CO₂ release;
 - ▶ Reduction of the energy to provide.

Industrial Context

- ▶ Cullet is mainly used for the production of container glass:

Germany	85 %	Belgium	96 %	France	75 %
Poland	57 %	Italy	78 %	Austria	87 %
United-Kingdom	66 %	Portugal	58 %	Spain	70 %
Sweden	99 %	Holland	83 %	Denmark	85 %

Table 1: Rates of glass recycling in Europe in 2015 [FEVE source].

- ▶ Advantages of introduction of cullet in raw materials:
 - ▶ Reductions of mineral resources;
 - ▶ Reduction of CO₂ release;
 - ▶ Reduction of the energy to provide.

What is the limitation to reach 100 % of cullet?

Industrial Context

How and why these bubbles are created?

1. Experimental set-up
2. Spatial distributions of nucleated bubbles
3. Bubble growth rate
4. Saturation and nucleation
5. Conclusion

1. Experimental set-up

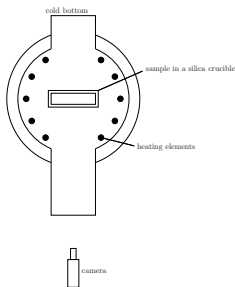


Figure 1: Sketch of HTO furnace.

SiO ₂	Na ₂ O	CaO	MgO	Al ₂ O ₃	SO ₃	Fe ₂ O ₃	FeO
72.4	13.85	8.88	3.74	0.73	0.22	0.055	0.014

Table 2: Composition of the **float glass** (wt %).

- ▶ Recording of the melting with 2 cameras (60 and 25 μm/px).

2. Spatial distributions of nucleated bubbles

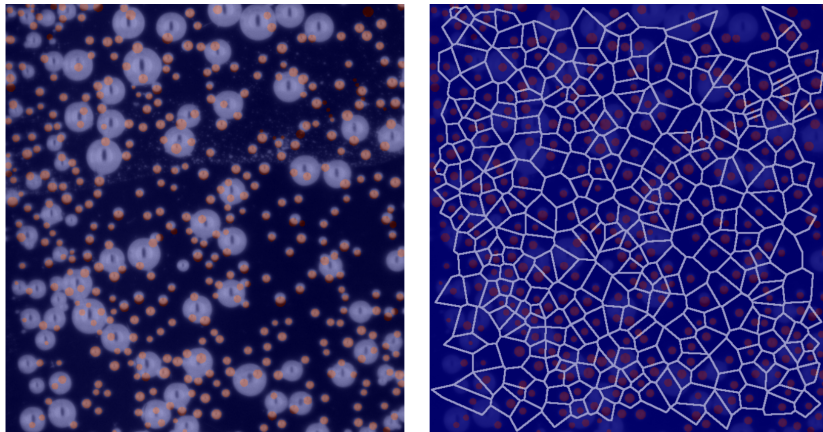


Figure 2: Detection of nucleation sites on each face of the crucible and Voronoï diagram of nucleation sites.

2. Spatial distributions of nucleated bubbles

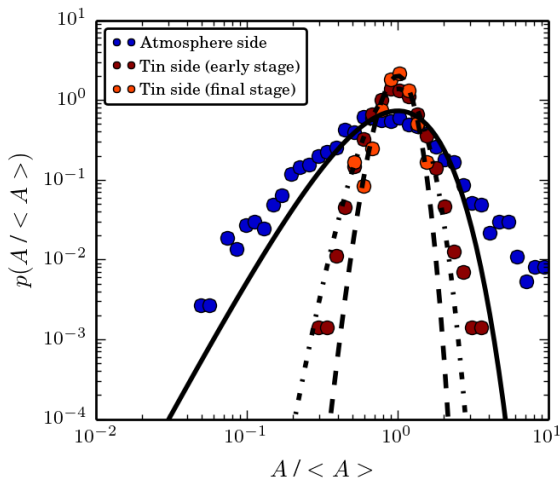


Figure 3: PDF of the area of Voronoï cells.

2. Spatial distributions of nucleated bubbles

- ▶ PDF can be described by the Gamma distribution:

$$f(x) = n^n x^{n-1} e^{-nx} / \Gamma(n), \quad (1)$$

with $x = \frac{A}{\langle A \rangle}$.

- ▶ Atmosphere side: $n = 3.5$;
- ▶ Tin side: $n = 12.2$ at the beginning and $n = 25.5$ at the end.
- ▶ For objects randomly distributed over a surface, $n = 7/2$ ¹.
- ▶ The disagreement on the tin side due to the **bubble coalescence**.

¹J.-S. Ferenc/Z. Néda: On the size distribution of Poisson Voronoi cells, in: *Physica A* 385.2 (2007), pp. 518–526.

2. Spatial distributions of nucleated bubbles

- ▶ Simulation population of bubbles undergoing coalescence:
 1. Population of 3000 “nuclei” distributed following a Poisson distribution over a square of 10^8 pixels;
 2. At each step, the closest “nuclei” are gathered at the barycentre position.

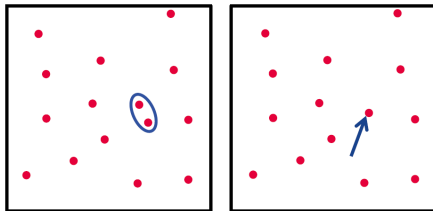


Figure 4: Coalescence between the closest nuclei.

3. Process is reiterated 500 to 1500 times.
4. “Numerical experiences” are repeated 500 times.

2. Spatial distributions of nucleated bubbles

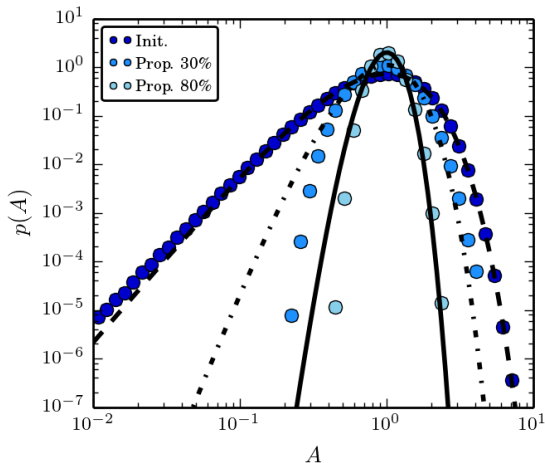


Figure 5: PDF of area of Voronoï cells obtained from the numerical simulations.

2. Spatial distributions of nucleated bubbles

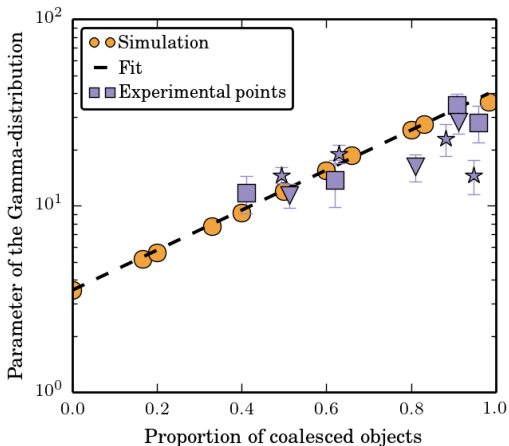


Figure 6: n vs. the proportion of coalesced objects.

$$n = \frac{7}{2} e^{2.47x}, \text{ with } x = \frac{d_0 - d}{d_0}. \quad (2)$$

2. Spatial distributions of nucleated bubbles

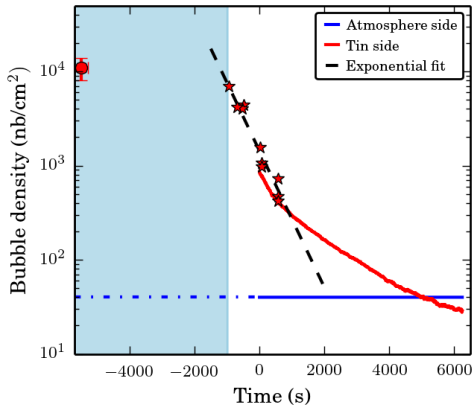


Figure 7: Bubble densities on the two sides of glass samples.

- ▶ In atmosphere side, $d_0 = 40$ nuclei/cm²;
- ▶ In tin side, $d_0 = 9300$ nuclei/cm² (230 times larger).

3. Bubble growth rate

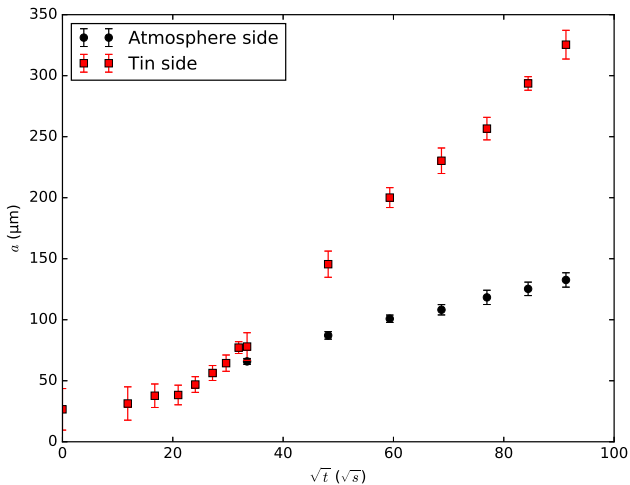
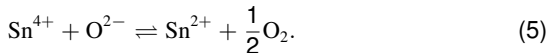
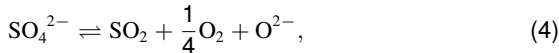
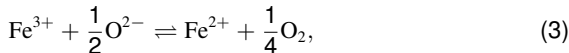


Figure 8: α (μm) vs. \sqrt{t} ($\sqrt{\text{s}}$) for bubbles on tin and atmosphere sides of molten glass samples.

3. Bubble growth rate

- ▶ Three redox couples are taken into account²:



- ▶ Gas contents (O_2 , SO_2 , H_2O , CO_2 & N_2) and bubble radius are determined by:

$$\frac{dn_{G_j}}{dt} = 4\pi a D_{G_j} (C_{G_j} - L_{G_j} P_{G_j}^{\beta_{G_j}}), \quad (6)$$

$$\frac{da}{dt} = \frac{a}{4\mu} \left(\sum_{i=1}^{N_g} P_{G_i} - P_l - \frac{2\gamma}{a} \right). \quad (7)$$

²F. Pigeonneau: Mechanism of mass transfer between a bubble initially composed of oxygen and molten glass, in: *Int. J. Heat Mass Transfer* 54 (2011), pp. 1448–1455.

3. Bubble growth rate

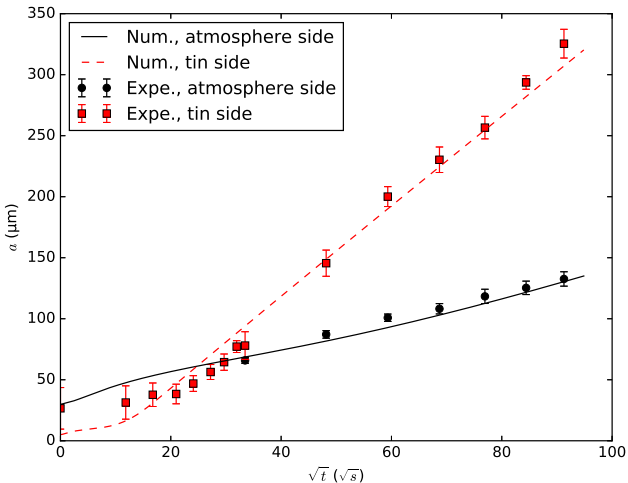


Figure 9: a (μm) vs. \sqrt{t} (\sqrt{s}) for bubbles on tin and atmosphere sides of molten glass samples.

3. Bubble growth rate

- ▶ In atmosphere side, $P_{O_2} = 1.3 \cdot 10^{-3}$ Pa; tin side, $P_{O_2} = 4.1 \cdot 10^{-4}$ Pa.
- ▶ Tin leads to a reduction of glass.
- ▶ Decrease of the SO_2 chemical solubility.

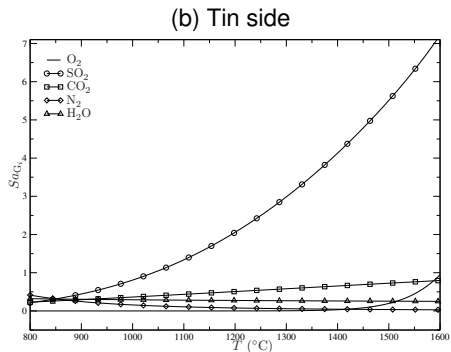
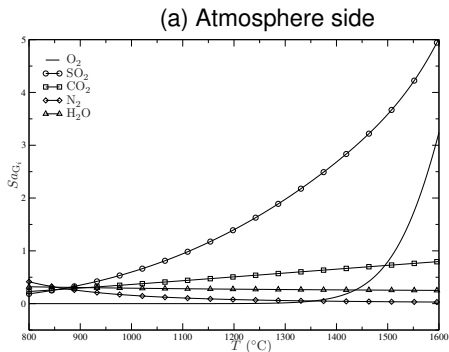


Figure 10: $Sa_{G_i} = C_{G_i} / (L_{G_i} P_i^{\beta_{G_i}})$ of the 5 gas species vs. T on both sides.

4. Saturation and nucleation

- ▶ The critical bubble size for nucleation in the case of multi-species is given by

$$a_{\text{cr}} = \frac{2\gamma}{\left(\sum_{i=1}^{N_g} Sa_{G_i}^{1/\beta_{G_i}} - 1 \right) P_l}, \quad (8)$$

$$Sa_{G_i} = \frac{C_{G_i}}{L_{G_i} P_l^{\beta_{G_i}}}. \quad (9)$$

- ▶ The supersaturation for N_g dissolved species is

$$\sigma = \sum_{i=1}^{N_g} Sa_{G_i}^{1/\beta_{G_i}} - 1. \quad (10)$$

4. Saturation and nucleation

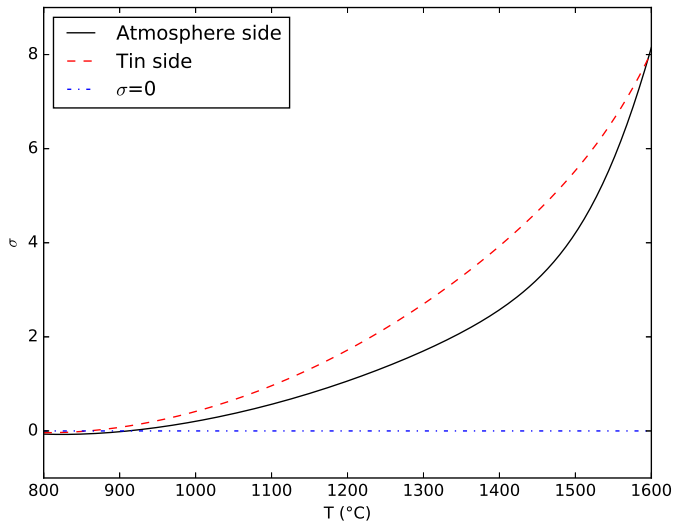


Figure 11: σ vs. T (°C) in atmosphere and tin sides.

5. Conclusion

- ▶ Remelting of cullet leads to a large bubble formation.
- ▶ Enhancements of the bubble nucleation and growth rate due to the tin pollution.
- ▶ The glass reduction on tin side is the main parameter controlling the bubble nucleation and the growth rate.
- ▶ Difficult to quantify the bubble nucleation rate (work in progress to improve the prediction).
- ▶ The 100 % of cullet is difficult to reach because the bubble creation persists and needs to introduce fining agents.
- ▶ See for more details³.

³D. Boloré/F. Pigeonneau: Spatial distribution of nucleated bubbles in molten glasses undergoing coalescence and growth, in: *J. Am. Ceram. Soc.* 101.5 (2018), pp. 1892–1905.